

The effect of disorder within the interaction theory of integer quantized Hall effect

S. E. Gulebaglan¹, G. Oylumluoglu², U. Erkarlan²,
A. Siddiki^{2,3} and I. Sokmen¹

¹Dokuz Eylül University, Physics Department, Tınaztepe Campus, 35100 İzmir, Turkey

²Muğla University, Physics Department, Faculty of Arts and Sciences, 48170-Kötekli, Muğla, Turkey

³Istanbul University, Faculty of Sciences, Physics Department, Vezneciler-Istanbul 34134, Turkey

E-mail: afifsiddiki@gmail.com

Abstract. We study effects of disorder on the integer quantized Hall effect within the screening theory, systematically. The disorder potential is analyzed considering the range of the potential fluctuations. Short range part of the single impurity potential is used to define the conductivity tensor elements within the self-consistent Born approximation, whereas the long range part is treated self-consistently at the Hartree level. Using the simple, however, fundamental Thomas-Fermi screening, we find that the long range disorder potential is well screened. While, the short range part is approximately unaffected by screening and is suitable to define the mobility at vanishing magnetic fields. In light of these range dependencies we discuss the extend of the quantized Hall plateaus considering *the* “mobility” of the wafer and the width of the sample, by re-formulating the Ohm’s law at low temperatures and high magnetic fields. We find that, the plateau widths mainly depend on the long range fluctuations of the disorder, whereas the importance of density of states broadening is less pronounced and even is predominantly suppressed. These results are in strong contrast with the conventional single particle pictures. We show that the widths of the quantized Hall plateaus increase with increasing disorder, whereas the level broadening is negligible.

This work focuses on the disorder effects on the integer quantized Hall effect within the screening theory. Since the early days of QHE, disorder played a very important role, however, interactions were completely neglected. Here we present our results which also includes interactions in a self-consistent manner and show that even without localization one can obtain the quantized Hall plateaus. We investigated different aspects of the impurity potential and suggested a criterion on mobility at high magnetic fields. We think that our work will shed light on the understanding of the QHE and is interest to condensed matter community. *Keywords:* Article preparation, IOP journals Submitted

1. Introduction

The integer quantized Hall effect (IQHE), observed at two dimensional charge systems (2DCS) subject to strong perpendicular magnetic fields B , is usually discussed within the single particle picture, which relies on the fact that the system is highly disordered [1, 2]. These quantized (spinnless) single particle energy levels are called the Landau levels (LLs) and the discrete energy values are given by $E_N = \hbar\omega_c(n + 1/2)$, where n is the Landau index and $\omega_c = eB/m^*c$ is the cyclotron frequency of an electron with an effective mass m^* ($\approx 0.067m_e$, m_e being the bare electron mass at rest) and c is the speed of light in vacuum. In single particle models the disorder plays several roles, such as Landau level broadening [3], leading to a finite longitudinal conductivity [4, 5], spatial localization [6] *etc.* Disorder can be created by inhomogeneous distribution of dopant ions which essentially generates the confinement potential [7] for the electrons. In the absence of disorder, the density of states are Dirac delta-functions $D(E) = \frac{1}{2\pi l^2} \sum_{N=0}^{\infty} \delta(E - E_N)$, where $l = \sqrt{\hbar/eB}$ is the magnetic length, and the longitudinal conductivity (σ_l) vanishes. For a homogeneous two dimensional electron system (2DES), by the inclusion of disorder and due to collisions, LLs become broadened. Therefore the longitudinal conductance becomes non-zero in a finite energy (in fact magnetic field) interval. Long range potential fluctuations generated by the disorder result in the so called *classical localization* [8], *i.e.* the guiding center of the cyclotron orbit moves along closed equi-potentials [9]. In contrast to the above mentioned bulk theories, the edge theories usually disregard the effect of disorder to explain the (quantized) Hall resistance R_H and accompanying (zero) longitudinal resistance R_L . However, the non-interacting edge theories still require disorder to provide a reasonable description of the transition between the plateaus. The Landauer-Büttiker approach (known as the edge channel picture) [10] and its direct Coulomb interaction generalized version, *i.e.* the non-self-consistent Chklovskii picture [11], also needs localization assumptions in order to obtain quantized Hall (QH) plateaus of finite width (see for a review *e.g.* Datta's book [12] and Ref. [9] for the estimates of plateau widths at the high disorder limit).

In contrast to above discussions very recent experimental [13, 14, 15, 16] and theoretical [17, 18] results point the incomplete treatment of the disorder potential and scattering mechanisms. Fairly recent theoretical approaches [19], the QH plateaus are obtained by the inclusion of direct Coulomb interaction self-consistently [20] and the effect of the disorder was handled via conductivity tensor elements [21], however, the source of the disorder and its properties was left unresolved [22]. Whereas, the influence of potential fluctuations on the QH plateaus were discussed briefly [23, 24].

This work provides a systematic investigation of the disorder potential and its influence on the quantized Hall effect including direct Coulomb interaction. The investigation is extended to realistic experimental conditions in determining the widths of the quantized Hall plateaus. We, essentially study the effect of disorder in two distinct regimes, namely the short range and the long range. The short range part is included to the density of states (DOS), thereby influences the widths of the current carrying

edge-states and the entries of the conductivity tensor. Whereas, the long range part is incorporated to the self-consistent calculations, which determines the extend of the plateaus in turn. In Sec 2 we introduce two types of single impurity potentials, namely the Coulomb and the Gaussian, and compare their range dependencies considering damping of the dielectric material. In the next step we discuss the *screened* disorder potential within a pure electrostatic approach, by considering an homogeneous two dimensional electron system (2DES) without an external magnetic field and show that the long range part is well screened, whereas the short range part is almost unaffected. Section 2.2 is devoted to investigate impurities numerically, where we solve the Poisson equation self-consistently in three dimensions. The numerical and analytical calculations are compared, considering the estimations of the disorder potential range and its variation amplitude. We finalize our discussion with Sec. 3, where we calculate the plateau widths under experimental conditions for different sample widths and mobilities.

2. Impurity potential

The disorder potential experienced by the 2DES, resulting from the impurities has quite complicated range dependencies. Since, the potential generated by an impurity is (i) *damped* by the dielectric material in between the impurity and the plane where the 2DES resides (ii) is screened by the homogeneous 2DES depending on the density of states, which changes drastically with and without magnetic field. It is common to theoreticians to calculate the conductivities from single impurity potentials, such as Lorentzian [19], Gaussian [25] or any other analytical functions [26, 27]. However, the landscape of potential fluctuations is also important to define the actual mobility of the sample at hand, in particular in the presence of an external magnetic field.

2.1. Pure Electrostatics

We first discuss the different range dependencies of the Coulomb and Gaussian donors, assuming open boundary conditions. Next, the effect of the spacer thickness on the disorder potential is discussed, namely the damping of the external (Coulomb) potential, and is compared with the Thomas-Fermi screening. The different damping/screening dependencies of the resulting potentials are discussed in terms of range.

The Coulomb potential presents long range part, which leads to long range fluctuations due to overlapping if several donors are considered. Whereas, the Gaussian potential decays exponentially on the length scale comparable with the separation thickness. Since the Gaussian potential is relatively short ranged, no overlapping of the single donor potentials occur. Hence, the external potential experienced by the electrons can be approximated to a homogeneous potential fairly good. Thus one can conclude that approximating the total disorder potential by Gaussians is not sufficient to recover the long range part. Similar arguments are also found in the literature [6, 9, 24]. In order to overcome the difference observed at the long range potential fluctuations

between the Coulomb and the Gaussian impurities, the following procedure is applied: First we calculate the total disorder potential considering many impurities then we perform a two-dimensional Fourier transformation of the Coulomb potential and make a back transformation keeping the first few momentum q components in each direction, hence only the long range part of the potential is left [24]. Then we add the long range part of the Coulomb potential to the potential created by donors, *i.e.* to the confinement potential. We take this as a motivation to simulate the short range part of the impurity potential by Gaussian impurities, and calculate the Landau level broadening and the conductivities, described within the self-consistent Born approximation (SCBA) [25].

Here we point to the effect of the spacer thickness on the impurity potential experienced in the plane of 2DES. It is well known from experimental and theoretical investigations that, if the distance between the electrons and donors is large, the mobility is relatively high and it is usually related with suppression of the short range fluctuations of the disorder potential. These results agree with the experimental observations of high mobility samples and are easy to understand from the z dependence of the Fourier expansion of the Coulomb potential,

$$V^{\vec{q}}(z) = \int d\vec{r} e^{-i\vec{q}\cdot\vec{r}} \sum_j^N \frac{e^2/\bar{\kappa}}{\sqrt{(\vec{r} - \vec{r}_j)^2 + z^2}} = \frac{2\pi e^2}{\bar{\kappa}q} e^{-|qz|} NS(\vec{q}), \quad (1)$$

where $S(\vec{q})$ contains all the information about the in-plane donor distribution and N is the total number of the ionized donors. We observe that if the spacer thickness is increased, the amplitude of the potential decreases rapidly. We also see that the short range potential fluctuations, which correspond to higher order Fourier components, are suppressed more efficiently.

Next, we discuss electronic screening of the external potential created by the donors discussed above. For a dielectric material the relation between the external and the screened potentials are given by,

$$V_{\text{scr}}^q = V_{\text{ext}}^q / \epsilon(q), \quad (2)$$

where $\epsilon(q)$ is the dielectric *function* and is given by $\epsilon(q) = 1 + \frac{2\pi e^2 D_0}{\bar{\kappa}|q|}$, with the constant 2D density of states $D_0 = m/(\pi\hbar^2)$ in the absence of an external B field, and is known as the Thomas-Fermi (TF) function. The simple linear relation above, together with the TF dielectric function essentially describes the electronic screening of the Coulomb potential given in Eq. 1, if there are sufficient number of electrons [9] ($n_{\text{el}} > 0.1 \cdot 10^{15} \text{ m}^{-2}$). Consider a case where the q component approaches to zero, then the external (damped) potential is well screened, hence the long range part of the disorder potential. Whereas, the short range part remain unaffected, *i.e.* high q Fourier components. Now we turn our attention to the second type of impurities considered, the Gaussian ones. As well known, the Fourier transform of a Gaussian is also of the form of a Gaussian, therefore, similar arguments also hold for this kind of impurity.

We should emphasize once more the clear distinction between the effect of the spacer on the external potential and the screening by the 2DES, *i.e.* via $\epsilon(q)$. The

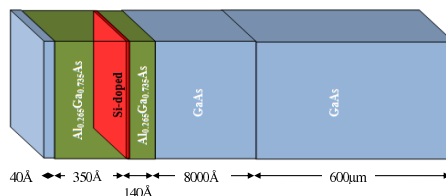


Figure 1. Schematic representation of the crystal, which we investigate numerically. The crystal is grown on a thick GaAs substrate, where the 2DES is formed at the interface of the AlGaAs/GaAs hetero-junction. The top AlGaAs layer is doped with Silicon 30 nm above the interface. The crystal is spanned by a 3D matrix ($128 \times 128 \times 60$).

former depends on the Fourier transform of the Coulomb potential and the important effect is the different decays of the different Fourier components (see Eq. 1), so that the short range part of the disorder potential is well dampened, whereas the latter depends on the relevant DOS of the 2DES and the screening is more effective for the long range part.

We continue our investigation by solving the 3D Poisson equation iteratively for randomly distributed single impurities, where three descriptive parameters (*i.e.* the number of impurities, the amplitude of the impurity potential and the separation thickness) are analyzed separately. Next, we discuss the long range parts of the potential fluctuations investigating the Coulomb interaction of the 2DES, numerically. The range is estimated from these investigations by performing Fourier analysis and is related to the samples used in experiments [15, 16] (Sec. 4).

2.2. 3D simulations

In the previous section we took a rather simple way to study the effect of interactions by assuming an homogeneous 2DES and screening is handled by the TF dielectric function. Here, we present our results obtained from a rather complicated numerical method. We solve the Poisson equation in 3D starting from the material properties of the wafer at hand, the typical material we consider is sketched in Fig. 1. Namely, using the growth parameters, we construct a 3D lattice where the potential and the charge distributions are obtained iteratively assuming open boundary conditions, *i.e.* $V(x \rightarrow \pm\infty, y \rightarrow \pm\infty, z \rightarrow \pm\infty) = 0$. For such boundary conditions, we chose a lattice size which is considerably larger than the region that we are interested in. We preserve the above conditions within a good numerical accuracy (absolute error of 10^{-6}). A fourth order grid approach [28] is used to reduce the computational time, which is successfully used to describe similar structures [29].

Figure 1 presents the schematic drawing of the hetero-structure which we are interested in. The donor layer is δ -doped by a density of $3.3 \times 10^{16} \text{ m}^{-2}$ (ionized) Silicon

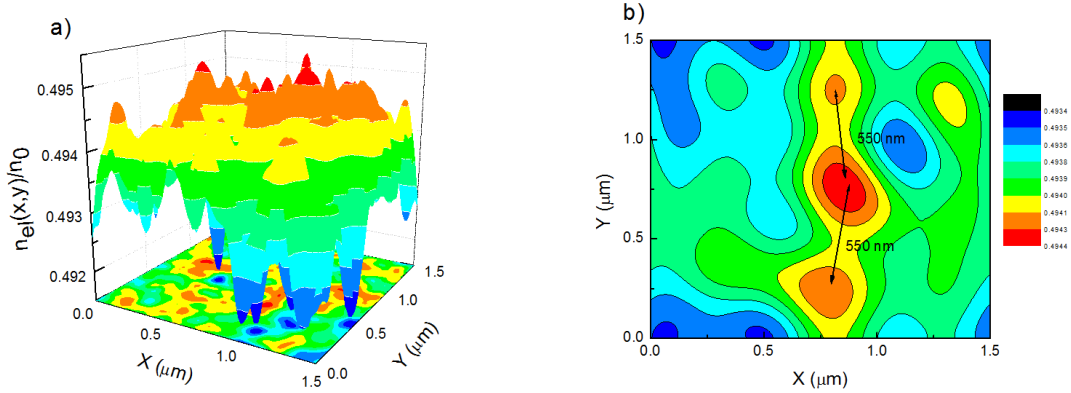


Figure 2. (a) Electron density fluctuation considering 3300 impurities 30 nm above the electron gas. (b) The long-range part, arrows are to guide the distance between two maxima. The calculation is repeated for 50 random distributions, which lead to a similar range.

atoms, ~ 30 nm above the 2DES, which provide electrons both for the potential well at the interface and the surface. It is worthwhile to note that most of the electrons ($\sim 90\%$) escape to the surface to pin the Fermi energy to the mid-gap of the GaAs. In any case, for such wafer parameters there are sufficient number of electrons ($n_{\text{el}} \gtrsim 3.0 \times 10^{15} \text{ m}^{-2}$) at the quantum well to form a 2DES. To investigate the effect of impurities we place positively charged ions at the layer where donors reside. From Eq. 1 we estimate the amplitude of the potential of a single impurity to be $\frac{e^2}{\kappa} \frac{V_{\text{imp}}}{z_D} = 0.033 \text{ eV}$ and assume that *some* percent of the ionized donors are generating the disorder potential, that defines the long range fluctuations. In our simulations we perform calculations for a unit cell with areal size of $1.5 \mu\text{m} \times 1.5 \mu\text{m}$ which contains 3.3×10^{16} donors per square meters, thus with 10 percent disorder we should have $N_I \sim 3300$ impurities. Figure 2a depicts the actual density distribution, when considering 3300 impurities, whereas Fig. 2b presents only the long range part of the density fluctuation. The arrows show the average distance between two maxima, which is calculated approximately to be 550 nm. To estimate an average range of the disorder potential, we repeated calculations for such randomly distributed impurities, where number of repetitions scales with $\sqrt{N_I}$. Such a statistical investigation, sufficiently ensembles the system to provide a reasonable estimation of the long range fluctuations. We also tested for larger number of random distributions, however, the estimation deviated less than tens of nanometers. We show our main result of this section in Fig. 3, where we plot the estimated long range part of the disorder potential considering various number of impurities N_I and impurity potential amplitude V_{imp} . Our first observation is that the long range part of the total potential becomes less when N_I becomes large, not surprisingly. However, the range increases nonlinearly while decreasing N_I , obeying almost an inverse square law and tend to saturate at highly disordered system. When fixing the distributions and N_I , and changing the amplitude of the impurity potential we observe that for large amplitudes the range can differ as

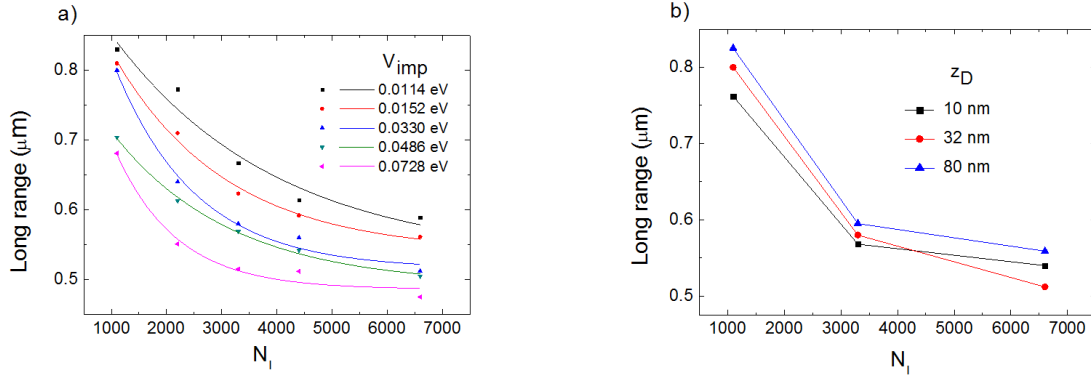


Figure 3. Statistically estimated range of the density fluctuations as a function of number of impurities, considering various impurity strengths (a) and spacer thicknesses (b). The calculations are done at zero temperature considering Coulomb impurities. The long range potential fluctuations become larger than the size of the unit cell if one considers less than %5 disorder.

large as 200 nm at all impurity densities. We found that for impurity concentration less than %3, the range of the potential is larger than the unit cell we consider, *i.e.* $R > 1.5\mu\text{m}$. In contrast to the long range part, the short range part is almost unaffected by the impurity concentration, however, is affected by the amplitude. Therefore, while defining the conductivities we will focus our investigation on V_{imp} . Another important result is that the estimates of long range fluctuations does not depend strongly on the spacer thickness, if one keeps the amplitude of single impurity potential amplitude fixed, Fig. 3b. All of the above numerical observations coincide fairly good with our analytical investigations in the previous section. However, the range dependency on the impurity concentration cannot be estimated with the analytical formulas given. We should also note that, similar or even complicated numerical calculations are present in the literature [6, 7]. A indirect measure of the screening effects on the potential can also be inferred by capacitance measurements, supported by the above calculation scheme in the presence of external field [14].

Next section is devoted to investigate the widths of the quantized Hall plateaus utilizing our findings. We consider mainly two “mobility” regimes, where the long range fluctuations is at the order of microns (high mobility) and is at the order of few hundred nanometers, low mobility. However, the amplitude of the total potential fluctuations will be estimated not only depending on the number of impurities but also depending on the spacer thickness, range and amplitude of single impurity potential.

3. Quantized Hall plateaus

The main aim of this section is to provide a systematic investigation of the quantized Hall plateau (QHP) widths within the screening theory of the IQHE [20], therefore here we summarize the essential findings of the mentioned theory. In calculating the

QHPs one needs to know local conductivities, namely the longitudinal $\sigma_1(x, y)$ and the transverse $\sigma_H(x, y)$. To determine these quantities it is required to relate the electron density distribution $n_{\text{el}}(x, y)$ to the local conductivities explicitly. Here we utilize the SCBA [25]. However, the calculation of the electron density and the potential distribution including direct Coulomb interaction is not straightforward, one has to solve the Schrödinger and the Poisson equations simultaneously. This is done within the Thomas-Fermi approximation which provides the following prescription to calculate the electron density

$$n_{\text{el}}(x, y) = \int dE D(E) \frac{1}{e^{(E_F - V(x, y))/k_B T} + 1}, \quad (3)$$

where $D(E)$ is the appropriate density of states calculated within the SCBA, where k_B is the Boltzmann constant and T temperature. The total potential is obtained from

$$V(x, y) = \frac{2e^2}{\bar{\kappa}} \int dx dy K(x, y, x', y') n_{\text{el}}(x, y), \quad (4)$$

and the Kernel $K(x, y, x', y')$ is the solution of the Poisson equation satisfying the boundary conditions to be discussed next.

In the following we assume a translation in variance in y -direction and implement the boundary conditions $V(-d) = V(d) = 0$ ($2d$ being the sample width), proposed by Chklovskii *et.al.* [11], such a geometry allows us to calculate the Kernel in a closed form. Hence, Eqs. (3) and (4) forms the self-consistency. For a given initial potential distribution, the electron concentration can be calculated at finite temperature and magnetic field, where the density of states $D(E)$ contains the information about the quantizing magnetic field and the effect of short range impurities. Here we implicitly assume that the electrons reside in the interval $-b < x < b$ (where, $d_l = |d-b|/d$ is called the depletion length), and is fixed by the Fermi energy, *i.e.* the number of electrons, hence donors. As a direct consequence of Landau quantization and the locally varying electrostatic potential, the electronic system is separated into two distinct regions, when solving the above self-consistent equations iteratively: i) The Fermi energy equals to (spin degenerate) Landau energy and due to DOS the system illustrates a metallic behavior, the compressible region, ii) The insulator like incompressible region, where E_F falls in between two consequent eigen-energies and no states are available [11, 30]. It is usual to define the filling factor ν , to express the electron density in terms of the applied B field as, $\nu = 2\pi l^2 n_{\text{el}}$. Since all the states below the Fermi energy are occupied the filling factor of the incompressible regions correspond to integer values (*e.g.* $\nu = 2, 4, 6, \dots$), whereas the compressible regions have non-integer values, due to partially occupied higher most Landau level. The spatial distribution and widths of these regions are determined by the confinement potential [11], magnetic field [31], temperature [32] and level broadening [19, 20]. For the purpose of the present work we fix the confinement potential profile by confining ourselves to the Chklovskii geometry and keeping the donor concentration (and distribution) constant. Moreover we perform our calculations at a default temperature given by $k_B T / E_F^0 = 0.02$, where E_F^0 is the

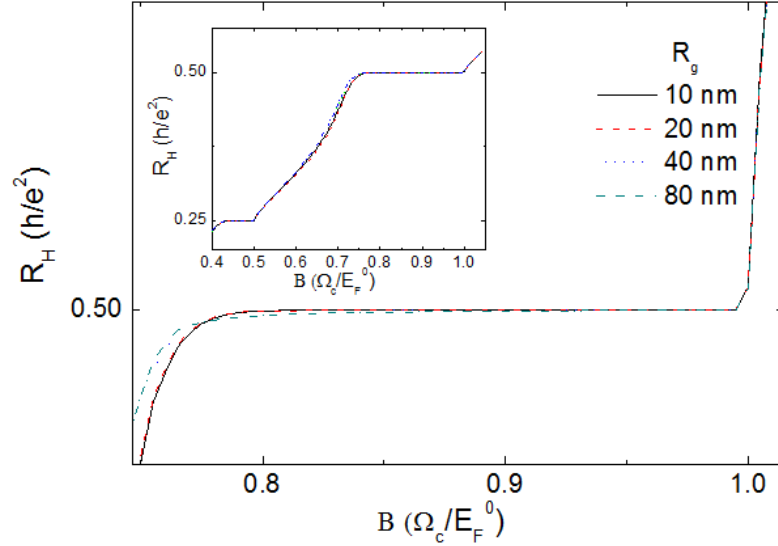


Figure 4. The Hall resistances versus magnetic field, calculated at default temperature and considering a 10 μm sample for different ranges of the single impurity potential. Inset depicts a larger B field interval, where $\nu = 4$ plateau can also be observed.

Fermi energy calculated for the electron concentration at the center of the sample and is typically similar to 10 meV.

The next step is to calculate the global resistances, *i.e.* the longitudinal R_L and Hall R_H resistances, starting from the local conductivity tensor elements. Such a calculation is done within a relaxed local model that relates the current densities $\mathbf{j}(x, y)$ to the electric fields $\mathbf{E}(x, y)$, namely the local Ohm's law:

$$\mathbf{j}(x, y) = \hat{\sigma}(x, y)\mathbf{E}(x, y). \quad (5)$$

The strict locality of the conductivity model is lifted by an spatial averaging process [20] over the quantum mechanical length scales and an averaged conductivity tensor $\hat{\sigma}(x, y)$ is used to obtain the global resistances. It should be emphasized that, such an averaging process also simulates the quantum mechanical effects on the electrostatic quantities. To be explicit: if the widths of the current carrying incompressible strips become narrower than the extend of the wave functions, these strips become “leaky” which can not decouple the two sides of the Hall bar and back-scattering takes place. Therefore, to simulate the “leakiness” of the incompressible strips we perform coarse-graining over quantum mechanical length scales.

Now let us relate the local conductivities with the local filling factors. Since the compressible regions behave like a metal within these regions there is finite scattering

$d_l = 70$ nm	$R_g = 10$ nm	20 nm	40 nm	80 nm
$2d = 2$ μm	0.120	0.120	0.100	0.050
3 μm	0.135	0.125	0.090	0.035
5 μm	0.140	0.115	0.070	0.020
8 μm	0.135	0.095	0.050	0.010
10 μm	0.130	0.085	0.040	0.010

leading to finite conductivity. In contrast, within the incompressible regions the back-scattering is absent, hence, the longitudinal conductivity (and simultaneously resistivity) vanishes. Therefore, all the imposed current is confined to these regions. The Hall conductivity, meanwhile is just proportional to the local electron density. The explicit forms of the conductivity tensor elements are presented elsewhere [20]. Having the electron density and local magneto-transport coefficients at hand, we perform calculations to obtain the widths of the quantized Hall plateaus utilizing the above described, microscopic model assisted by the local Ohm's law at a fixed external current I . Further details of the calculation scheme is reviewed in Ref. [23].

3.1. Single impurity potentials: Level broadening and conductivities

Since the very early days of the charge transport theory, collisions played an important role. Such a scattering based definition of conduction also applies for the system at hand, *i.e.* a two-dimensional electron gas subject to perpendicular magnetic field. Among many other approaches [33, 19, 27] the SCBA emerged as a reasonable model to describe the DOS assuming Gaussian impurities, considering short range scattering. A single impurity has two distinct parameters that represents the properties of the resulting potential, the range R_g (at the order of separation thickness) and the amplitude of the potential (in relevant units), \tilde{V}_{imp} . However, these two parameters are not enough to define the widths of the Landau levels (Γ), another important parameter is the number of the impurities, N_I . In the previous section we have already investigated these three parameters in scope of potential landscape, now we utilize our findings to define the level widths and the conductivities. It is more convenient to write the single impurity potential of the form,

$$V_g(r) = \frac{\tilde{V}_{\text{imp}}}{\pi R_g^2} \exp\left(-\frac{r^2}{R_g^2}\right). \quad (6)$$

Together with the impurity concentration, the relaxation time is defined as $\tau_0 = \frac{\hbar^3}{N_I \tilde{V}_{\text{imp}}^2 m^*}$ and in the limit of delta impurities (*i.e.* $R_g \rightarrow 0$) the Landau level width Γ takes the form $\Gamma = \sqrt{\frac{4N_I \tilde{V}_{\text{imp}}^2}{2\pi l^2}}$. It is useful to define the impurity strength parameter to investigate the effect of disorder by

$$\gamma_I^2 = (\Gamma/\hbar\omega_c)^2 = \frac{2N_I \tilde{V}_{\text{imp}}^2 m}{\pi \hbar^3 \omega_c}, \quad (7)$$

$d_l = 150 \text{ nm}$	$R_g = 10 \text{ nm}$	20 nm	40 nm	80 nm
2d= 2 μm	0.140	0.140	0.125	0.075
3 μm	0.160	0.150	0.120	0.055
5 μm	0.180	0.150	0.095	0.035
8 μm	0.180	0.130	0.070	0.020
10 μm	0.175	0.120	0.060	0.015

Table 1. The $\nu = 2$ plateau widths obtained at default temperature for two depletion lengths d_l (left 75 nm, right 150 nm), while $\gamma_I = 0.05$ is fixed (defined in Eq. 7 and the related text below). The widths are given in units of $\hbar\omega_c/E_F^0 = \Omega_c/E_F^0$.

given in units of magnetic energy $\hbar\omega_c = \frac{\hbar e B}{m} = \Omega_c$ and as a normalization parameter we fix the magnetic energy at 10 T.

At this point we would like to make a remark on the concepts short/long range impurities and short/long range potential fluctuations, which is commonly mixed. By short range impurity potential we mean that $R_g \lesssim l$, however, by short range potential fluctuation a length scale of the order of 200 – 300 nm is meant. The long range impurity potential corresponds to $R_g > l$ and long range potential fluctuation is of the order of micrometers. Thus, when considering short range impurities the potential fluctuations may be long range, if N_I is not large ($< \%5$ of the donor concentration). We have also observed that, the long-range potential fluctuations are more efficiently screened by the 2DES and their range can be at the order of 500 nm at most, when assuming large impurity concentration, *i.e.* $N_I > \%10$. In light of the above findings and formulation we now investigate the widths of the quantized Hall plateaus. Figure 4 presents the calculated Hall resistances at a fixed temperature for typical single impurity ranges. We observe that, when increasing R_g the plateau widths remain approximately the same, with a small variation, which is in contrast to the experimental findings, *i.e.* if the system is low mobility (small $R_g \Rightarrow$ highly broadened DOS) the plateau are larger. In fact changing R_g from 10 nm to 20 nm should increase the zero B field mobility almost an order of magnitude, when fixing the other parameters (see *e.g* table I of Ref. [20]). The contradicting behavior is due to the fact that the levels become broader when increasing the single impurity range, therefore the incompressible strips become narrower, which results in a narrower plateau. However, the long range potential fluctuations are completely neglected, therefore the effect(s) of disorder on the quantized Hall plateaus cannot be described in a complete manner. To investigate the effect of the single impurity range we systematically calculated the plateau widths; table 1 depicts the calculated widths of the Hall plateaus considering different sample widths, depletion lengths, filling factors and R_g . One sees that the plateau widths are affected by the increase of impurity range, however, in a completely wrong direction, *i.e.* plateaus become narrower when decreasing the mobility. As we show in the next section, it is not sufficient to describe mobility only considering the range of a single impurity. Moreover, we also show that the other two parameters defining $B = 0$ mobility are either

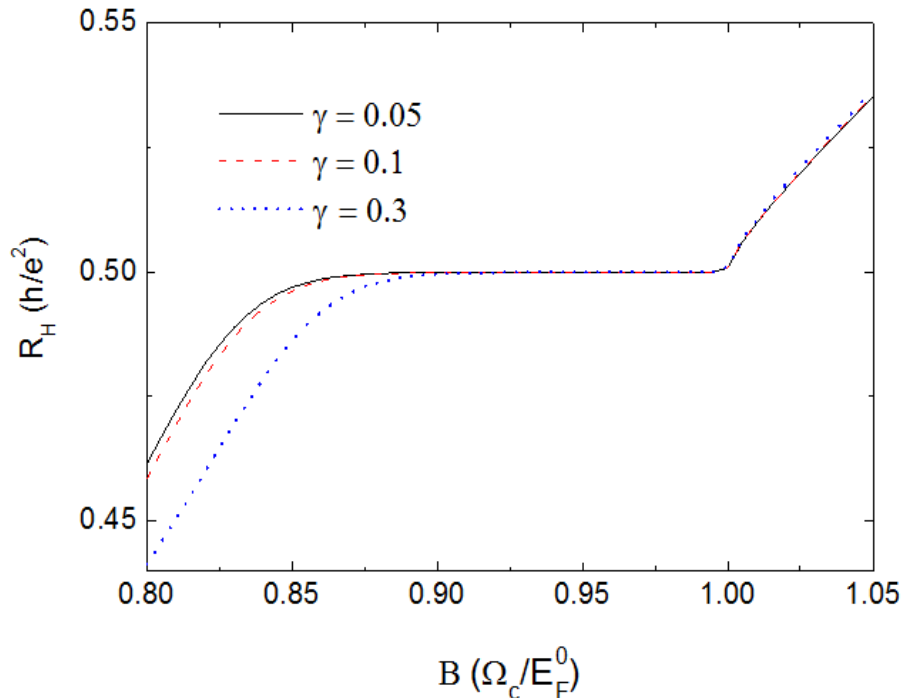


Figure 5. The calculated Hall resistances at default temperature assuming a $5 \mu\text{m}$ sample considering three characteristic value of broadening parameter. The lowest mobility ($\gamma_I=0.3$) shows the narrowest plateau.

not important or behaves in the opposite direction when calculating the resistances.

Next we investigate the effect of the remaining two parameters, \tilde{V}_{imp} and N_I . However, these two parameters both effect the level width simultaneously, thereby the widths of the incompressible strips. Hence, one cannot to distinguish their influence on the QHPs separately. Typical Hall resistances are shown in Fig. 5 calculated at default temperature considering different impurity parameters. Similar to the range parameter, we observe that the plateau widths become narrower when the mobility is low, which also points that our single particle based level broadening calculations are not in the correct direction. Such a behavior is easy to understand, when we decrease the mobility either by increasing the impurity concentration or by the amplitude of the impurity potential, the Landau levels become broader due to collisions. This means that, both the energetic and spatial gap between two consequent levels is reduced, hence the resulting incompressible strips are also narrower and fragile even at low temperatures. A detailed investigation on the incompressible widths depending on impurity parameters are reported in Ref. [19]. It is known that if there exists an incompressible strip wider than the Fermi wavelength the system is in the quantized Hall regime [20], therefore, if the gap is reduced the incompressible strips are smeared, thus the quantized Hall plateau vanish. As a general remark on the single particle theories, we should note that such a

reduced gap is also a gross problem for the non-interacting models [34, 35, 36], however, one can overcome this discrepancy by making localization assumptions [1]. Namely, one assumes that even within the broadened Landau levels there are states, which are localized, therefore electrons cannot contribute to transport. Hence, although the gap is small (levels are broad) these localized states serves as a reasonable candidate to explain the low mobility behavior. In the early days of IQHE it was a great challenge to describe and observe these localized states [3]. Recent experiments [37, 38, 15, 39] show clearly that, the localization assumptions are not relevant in all the cases, *i.e.* narrow and high mobility samples. Moreover, the universal behavior of the localization length dictated by these theories fail [40]. An explicit treatment of the activation energy [41] and critical exponents are left to an other publication.

3.2. Size effects on plateau widths

Another important parameter in defining the plateau widths is the depletion length d_l . The slope of the confinement potential close to the edges essentially determines the widths of the incompressible strips [11], which in turn determines the plateau widths. In Fig. 6 we show the $\nu=2$ plateau calculated for two different depletion lengths, we see that for the larger depletion the plateau is more extended. Since, the larger the depletion is, the smoother the electron density is. Therefore, resulting incompressible strips are wider, hence the plateau. Such an argument will fail if one considers a highly disordered large sample, which we discuss in Sec. 3.3. Next, we compare the plateau widths of different sample sizes while keeping constant the disorder parameters and depletion length. Figure 6 depicts the sample size dependency of $\nu = 2$ plateau width. It is seen that the larger samples present wider plateaus, if the magnetic field is normalized with the center Fermi energy, E_F^0 . One can understand this by similar arguments given above, *i.e.* if the sample is narrow the variation of the confinement potential is stronger, therefore the incompressible strips become narrower, hence, the plateaus. The discrepancy between the experimental results and the screening theory of the IQHE is solved if one considers not only the single impurity potentials but also the overall *disorder* potential landscape generated by the impurities. In the next part of this section, we investigate the effect of the long range potential fluctuations on the quantized Hall plateaus and find that, when the mobility is reduced the plateaus become wider and stable, as it is observed in many experiments, (see *e.g.* Refs. [42, 15, 16]).

3.3. Many many impurities: Potential fluctuations

So far we have investigated the effect of single impurity potentials on the overall potential landscape in Sec. 2.2 and on the widths of the plateaus in Sec. 3.1. We have seen that, at high impurity concentration the overall potential fluctuates over a length scale of couple of hundred nanometers, whereas for low N_I concentration such length scale can be as large as micrometers. Now we include the effect of this long range potential fluctuations *into* our screening calculations via modulation potential defined

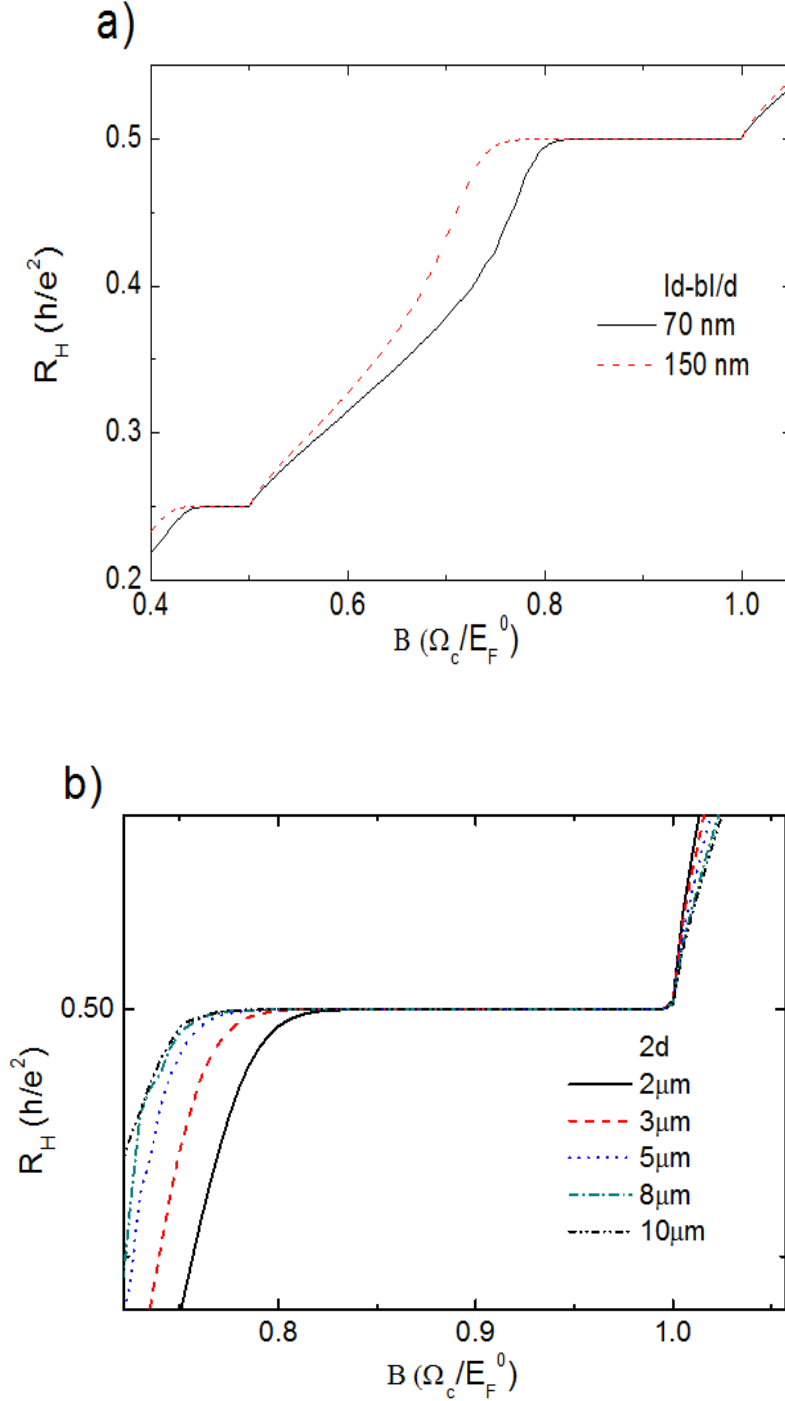


Figure 6. a) The calculated Hall resistances at a large B interval at default temperature, setting $2d = 5 \mu\text{m}$, $R_g = 20 \text{ nm}$ and $\gamma_I = 0.05$, while changing the depletion length. It is clearly seen that depletion length is much more important than the single impurity parameters in determining the plateau widths. (b) The direct comparison of the plateau widths considering different sample sizes. The impurity parameters and depletion lengths are kept constant. Calculations are done at $k_B T/E_F^0 = 0.02$, whereas the donor density is $4 \times 10^{15} \text{ m}^{-2}$ for all sample sizes.

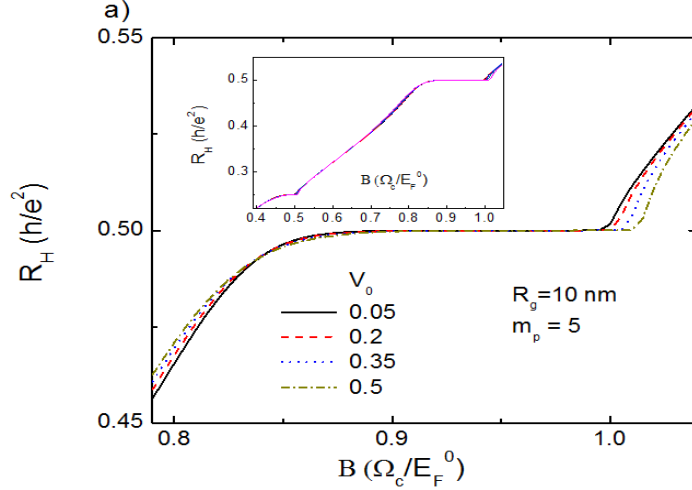


Figure 7. Self-consistently obtained Hall resistances for a modulated system considering a sample of $3 \mu\text{m}$. The depletion lengths and other single impurity parameters are kept fixed, whereas the parity of the modulation period is set 5.

as $V_{\text{mod}}(x) = V_0 \cos(\frac{2\pi x m_p}{2d})$ where, the modulation period m_p , is chosen such that the boundary conditions are preserved. At the moment, we consider two modulation periods regardless of the sample width and vary the amplitude of the modulation potential. In the next section, however, we select these two parameters from our estimations obtained in Sec. 2 and Sec. 2.2.

Figure 7 depicts the self-consistently calculated Hall resistances, considering different modulation amplitudes V_0 for a fixed sample width ($2d = 3 \mu\text{m}$) and $m_p = 5$. We observe that, the plateaus become wider from the high B field side, when V_0 is increased, *i.e.* mobility is reduced. Such a behavior is now consistent with the experimental findings. Since the QHPs occur whenever an incompressible strip is formed (somewhere) in the sample and the modulation forces the 2DES to form an incompressible strip at a higher magnetic field, therefore the plateau is also extended up to higher field compared with the (approximately) non-modulated calculation, $V_0/E_F^0 < 0.1$.

Our investigation of the impurities lead us to conclude that, one has to define mobility at high magnetic fields also taking into account screening effects in general and furthermore also the geometric properties of the sample such as the width and depletion length. As an example if we consider an impurity concentration of $\approx 1\%$ the long range part of the potential fluctuation can be approximated to 900 nm . However, note that the amplitude of this fluctuation varies between $5\% - 25\%$ of the Fermi energy, considering different separation thicknesses, therefore the wafer changes from low mobility to intermediate one. Another important parameter is the number of modulations within the system: a sample with an extend of $2 \mu\text{m}$ and $V_0/E_F = 0.1$

mobility	m_p (10 μm)	m_p (2 μm)	V_0/E_F^0
low	19-20	5-6	0.5
intermediate 1	9-10	2-3	0.5
intermediate 2	19-20	5-6	0.05
high	9-10	2-3	0.05

Table 2. A qualitative comparison of the mobility in the presence of magnetic field also taking into account self-consistent screening. Mobility also depends on the size of the sample when screening is also considered.

is a high mobility sample with the same m_p (only 2 maximum), however, sample with a width of 10 μm is low mobility (10 maximum). In the next section we study the plateau widths of different mobility samples, while keeping constant the extend and the amplitude of long range potential fluctuations (*i.e.* V_0 and m_p) and short range impurity parameters (\tilde{V}_{imp} , N_I and R_g) under experimental conditions.

4. Discussion: Comparison with the experiments

In this final section, we harvest our findings of the previous sections to make quantitative estimations of the plateau widths, considering narrow gate defined samples. Our aim is to show the qualitative and quantitative differences between “high” and “low” mobility samples, by taking into account properties of the single impurity potentials and the resulting disorder potential. The experimental realizations of these samples are reported in the literature [15, 16]. We estimated in Sec. 2.2 that, the range of the potential fluctuations is $\lesssim 500$ nm for low mobility ($N_I > 3300$) and is $\gtrsim 1$ μm at high mobility. Therefore, the modulation period is chosen such that many oscillations correspond to low mobility, and few oscillations correspond high mobility. As an specific example let us consider a 10 μm sample, for the low mobility we choose $m_p = 19 - 20$ and for the high mobility m_p is taken as 9 or 10. The amplitude of the disorder potential is damped to %50 of the Fermi energy when considering the effect of spacer thickness, however, including screening this amplitude is further reduced to few percents. In light of this estimations the low mobility will be presented by a modulation amplitude of $V_0/E_F^0 = 0.5$, whereas high mobility corresponds to $V_0/E_F^0 = 0.05$. Therefore, we have 4 different combinations of the disorder potential parameters yielding four different mobilities considering two sample widths, as tabulated in table 2. The second important aspect of the disorder is the single impurity parameters, for low mobility set we choose $R_g = 20$ nm and $\gamma_I = 0.3$, whereas for high mobility $R_g = 10$ nm and $\gamma_I = 0.05$ is set. Remember that, the range of the single impurity is much less important than γ_I in determining the plateau width (see sec. 3.1).

Figure 8 summarizes our results considering above discussed mobility regimes for two different sample widths. In Fig. 8a, we show the calculated Hall resistances for a sample of 10 microns with the highest mobility (solid (black) line) and intermediate

1 mobility (broken (red) line). The solid line is the highest mobility since the range of the fluctuations are at the order of $1 \mu\text{m}$ and the amplitude of the modulation potential is five percent of the Fermi energy. The broken line presents the intermediate mobility considering a modulation amplitude of fifty percent. We observe that the lower mobility wafer presents a larger quantized Hall plateau, which is now in complete agreement with the experimental results. Moreover, our calculation scheme is free of localization assumptions in contrast to the known literature and we only considered a very limited level broadening, *i.e.* $\gamma_I = 0.05$. In fact our results also hold for Dirac-delta Landau levels, however, for the sake of consistency we choose the broadening parameters according to the selected disorder parameters. In Fig. 8c, we show two curves for even lower mobilities, the solid line corresponds to the intermediate 2 case, whereas the broken line is the lowest mobility considered here. The potential fluctuation range (*i.e.* the modulation period) is chosen to present the low mobility wafer. We again see that for the lowest mobility the quantized Hall plateau is enlarged considerably from both edges of the plateau. These results explicitly show that the quantized Hall plateaus become broader if one strongly modulates the electronic system by long range potential fluctuations, either by changing the range *or* the amplitude of the modulation. Similar results are also obtained for a relatively narrower sample $2d = 3 \mu\text{m}$, Fig. 8b and 8d, however, we see that decreasing the range of the potential fluctuation is more efficient in enlarging the quantized Hall plateaus when compared to the effect of the amplitude of the modulation.

The last interesting investigation is on the parity of the modulation period, *i.e.* whether m_p is odd or even. Figure 9 presents the different behavior when considering even (a) or odd (b) periods. Here, all the disorder parameters are kept fixed, other than the parity. We see that for the even parity the plateau is shifted towards the high field edge, both for $\nu = 2$ and 4, whereas for the odd parity the plateau is enlarged from both sides. This tendency is also observed for the larger sample (not shown here). We attribute this behavior again to the formation of the incompressible strips, however, this time only to the one residing at the center of the sample, *i.e.* the bulk incompressible strip. The picture is as follows: If the maxima of the modulation potential is at the center of the sample, the incompressible strip is formed at a higher magnetic field value, whereas, the edge incompressible strips become narrower at the lower field side. Hence, due to the larger incompressible strip at the bulk of the sample the plateau is shifted to the higher field, in contrast, due to the narrower (compared to the unmodulated system) edge strips the plateau is cut off at higher fields. Since, the edge incompressible strip becomes narrower than the extend of the wave function. For the odd parity, the edge incompressible strips become wider, therefore, the plateau extends to the lower B fields. The enhancement at the high field edge results from the two maximum in the proximity of the center. For a better visualization of the incompressible strip distribution we suggest reader to look at Fig.2 of Ref. [24] and Fig.1 of Ref. [43]. Such a shift of the quantized Hall plateaus is also reported in the literature [42] and is attributed to the asymmetrical density of states due to the acceptors in the system [44]. We claim that,

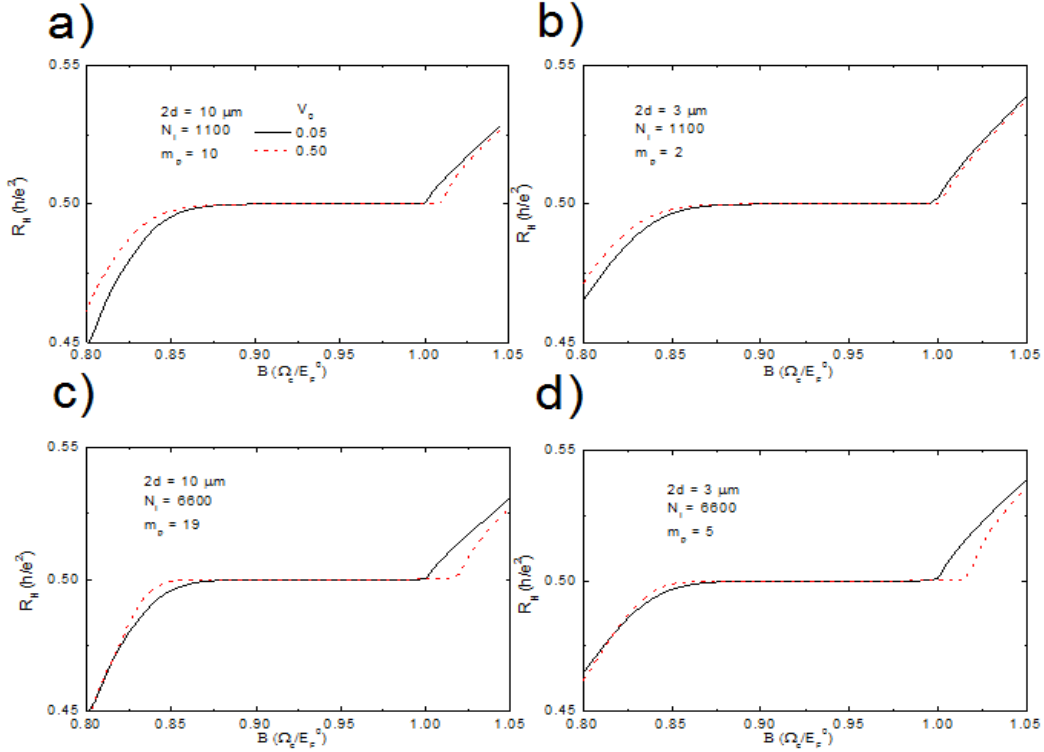


Figure 8. Line plots of the Hall resistance as a function of magnetic field considering two sample widths ($2d = 10 \mu\text{m}$ left panels, $2d = 3 \mu\text{m}$ right panels) and impurity concentrations ($\sim 3\%$ (a) and (b), $\sim 20\%$ (c) and (d)). Here the single impurity parameters are calculated from Eq. 7, otherwise other parameters are the same.

the shift due to the modulation parity change observed in our calculations overlap with their findings. Note that in our calculations we only consider symmetric DOS, however, replacing a maxima with a minima at the confinement potential corresponds to the acceptor behavior of the dopants. A systematic experimental investigation is suggested to understand the underlying physical mechanism, where the system is doped with small number of acceptors.

5. Conclusion

In this work we tackled with the long standing and widely discussed question of the effect of disorder on the quantized Hall plateaus. The distinguishing aspect of our approach relies on the separate treatment of the long and short range of the disorder potential. We show that assuming Gaussian impurities is not sufficient to describe long range potential fluctuations, however, is adequate to give a prescription in defining the density of states broadening and conductivities. The discrepancy in handling the long range potential fluctuations is cured by the inclusion of a modulation potential to the self-consistent calculations. We estimated the range of these fluctuations from our analytical and numerical calculations considering the effect of dielectric spacer and the screening of the

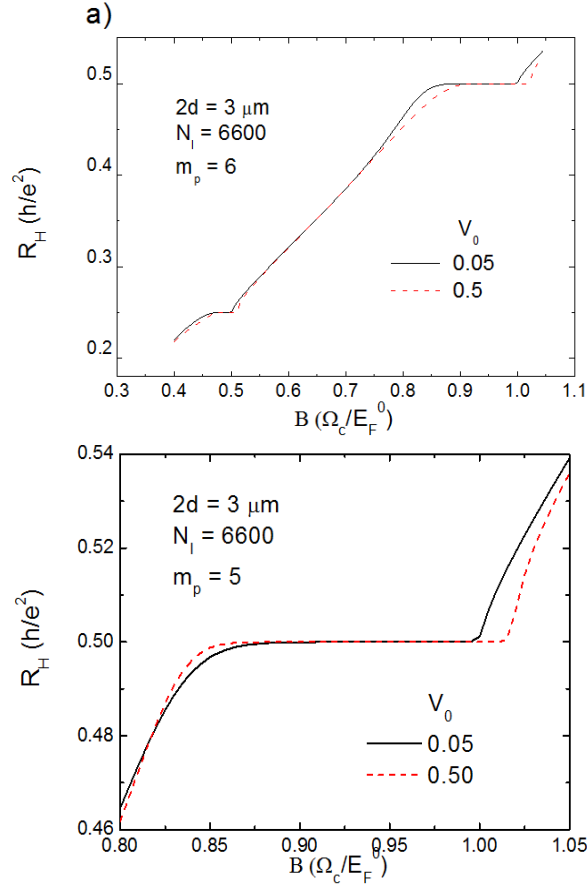


Figure 9. Even-odd parity dependency of the Hall plateaus at high impurity concentration. (a) corresponds to a “acceptor” doped wafer, whereas in (b) the ionized impurities are positively charged.

2DES. It is observed that spacer damps the short range fluctuations effectively, whereas the direct Coulomb interaction is dominant in screening the long range fluctuations. Utilizing the estimations of the range and the amplitude of potential fluctuations, we classified mobility in four groups and calculated the Hall resistances within the screening theory of the quantized Hall effect. We found that the Hall plateaus are wider when decreasing the mobility, not surprisingly. However, the most important point of our theory is that, we do not consider any localization assumptions, still obtain correct behavior of the plateau widths. We show that $B = 0$ and/or short range impurity defined mobility is not adequate to describe the actual mobility at high magnetic fields, moreover, one has to include geometrical properties of the sample at hand.

A natural persecutor theoretical investigation of the present work should deal with the activated behavior of the longitudinal resistance within the screening theory. As it is well known, the properties of the localized states, *e.g.* the localization length, is usually obtained from the activation experiments [45]. Moreover, spin generalization of the screening theory [46] is necessary to describe and investigate odd integer quantized plateaus also considering level broadening, namely disorder.

Acknowledgments

One of the authors (A.S.) would like to thank E. Ahlswede, S. C. Lok and J. Weiss for the enlightening discussions on the disorder from “an experimentalist” point of view. The Authors acknowledges, the Feza-Grsey Institute for supporting the III. Nano-electronic symposium, where this work has been conducted partially and would like to acknowledge the Scientific and Technical Research Council of Turkey (TUBITAK) for supporting under grant no 109T083.

References

- [1] B. Kramer, S. Kettmann, and T. Ohtsuki. Localization in the quantum hall regime. *Physica E*, 20:172, 2003.
- [2] L. Schweitzer, B. Kramer, and A. MacKinnon. Selective probing of ballistic electron orbits in rectangular antidot lattices. *Z. Physik B*, 59:379, 1985.
- [3] W. Cai and C. S. Ting. Screening effect on the landau-level broadening for electrons in gaas-gaalas heterostructures. *Phys. Rev. B*, 33:3967, 1986.
- [4] T. Ando and Y. Uemura. *J. Phys. Soc. Japan*, 36:959, 1974.
- [5] T. Ando, Y. Matsumoto, and Y. Uemura. *J. Phys. Soc. Japan*, 39:279, 1975.
- [6] J. A. Nixon and J. H. Davies. Potential fluctuations in heterostructure devices. *Phys. Rev. B*, 41:7929–7932, April 1990.
- [7] M. Stopa and Y. Aoyagi. Effect of donor layer ordering on the formation of single mode quantum wires. *Physica B Condensed Matter*, 227:61–64, September 1996.
- [8] M. M. Fogler and B. I. Shklovskii. Resistance of a long wire in the quantum hall regime. *Phys. Rev. B.*, 50:1656, 1994.
- [9] A. L. Efros. Non-linear screening and the background density of 2deg states in magnetic field. *Solid State Commun.*, 67:1019, 1988.
- [10] M. Büttiker. Four-terminal phase-coherent conductance. *Phys. Rev. Lett.*, 57:1761, 1986.
- [11] D. B. Chklovskii, B. I. Shklovskii, and L. I. Glazman. Electrostatics of edge states. *Phys. Rev. B*, 46:4026, 1992.
- [12] S. Datta. In *Electronic Transport in Mesoscopic Systems*, Cambridge, 1995. University press.
- [13] N. Ruhe, J. I. Springborn, C. Heyn, M. A. Wilde, and D. Grundler. Simultaneous measurement of the de Haas-van Alphen and the Shubnikov-de Haas effect in a two-dimensional electron system. *Phys. Rev. B*, 74(23):235326–+, December 2006.
- [14] Jiri J Mares, Afif Siddiki, Dobroslav Kindl, Pavel Hubik, and Jozef Kristofik. Electrostatic screening and experimental evidence of a topological phase transition in a bulk quantum hall liquid. *New Journal of Physics*, 11(8):083028, 2009.
- [15] J. Horas, A. Siddiki, J. Moser, W. Wegscheider, and S. Ludwig. Investigations on unconventional aspects in the quantum Hall regime of narrow gate defined channels. *Physica E Low-Dimensional Systems and Nanostructures*, 40:1130–1132, March 2008.
- [16] A. Siddiki, J. Horas, J. Moser, W. Wegscheider, and S. Ludwig. Interaction mediated asymmetries of the quantized Hall effect. *ArXiv e-prints:0905.0204[cond-mat.mes-hall]*, May 2009.
- [17] E. H. Hwang and S. Das Sarma. Limit to two-dimensional mobility in modulation-doped GaAs quantum structures: How to achieve a mobility of 100 million. *Phys. Rev. B*, 77(23):235437–+, June 2008.
- [18] S. J. MacLeod, K. Chan, T. P. Martin, A. R. Hamilton, A. See, A. P. Micolich, M. Aagesen, and P. E. Lindelof. Role of background impurities in the single-particle relaxation lifetime of a two-dimensional electron gas. *Phys. Rev. B*, 80(3):035310–+, July 2009.
- [19] K. Güven and R. R. Gerhardts. Self-consistent local-equilibrium model for density profile and

- distribution of dissipative currents in a hall bar under strong magnetic fields. *Phys. Rev. B*, 67:115327, 2003.
- [20] A. Siddiki and R. R. Gerhardtts. Incompressible strips in dissipative hall bars as origin of quantized hall plateaus. *Phys. Rev. B*, 70:195335, 2004.
- [21] A. Siddiki. Self-consistent coulomb picture of an electron-electron bilayer system. *Phys. Rev. B*, 75:155311, 2007.
- [22] A. Siddiki and R. R. Gerhardtts. The interrelation between incompressible srtips and quantized hall plateaus. *Int. J. Mod. Phys. B*, 18:3541, 2004.
- [23] R. R. Gerhardtts. The effect of screening on current distribution and conductance quantisation in narrow quantum Hall systems. *Phys. Stat. Sol.b*, 245:378, January 2008.
- [24] A. Siddiki and R. R. Gerhardtts. Range-dependent disorder effects on the plateau-widths calculated within the screening theory of the iqhe. *Int. J. of Mod. Phys. B*, 21:1362, 2007.
- [25] T. Ando, A. B. Fowler, and F. Stern. Electronic properties of two-dimensional systems. *Rev. Mod. Phys.*, 54:437, 1982.
- [26] T. Champel, S. Florens, and L. Canet. Microscopics of disordered two-dimensional electron gases under high magnetic fields: Equilibrium properties and dissipation in the hydrodynamic regime. *Phys. Rev. B*, 78(12):125302–+, September 2008.
- [27] T. Kramer. a Heuristic Quantum Theory of the Integer Quantum Hall Effect. *International Journal of Modern Physics B*, 20:1243–1260, 2006.
- [28] A. Weichselbaum and S. E. Ulloa. Potential landscapes and induced charges near metallic islands in three dimensions. *Phys. Rev E*, 68(5):056707–+, November 2003.
- [29] S. Arslan, E. Cicek, D. Eksi, S. Aktas, A. Weichselbaum, and A. Siddiki. Modeling of quantum point contacts in high magnetic fields and with current bias outside the linear response regime. *Phys. Rev. B*, 78(12):125423–+, September 2008.
- [30] A. Siddiki and R. R. Gerhardtts. Thomas-fermi-poisson theory of screening for laterally confined and unconfined two-dimensional electron systems in strong magnetic fields. *Phys. Rev. B*, 68:125315, 2003.
- [31] K. Lier and R. R. Gerhardtts. Self-consistent calculation of edge channels in laterally confined two-dimensional electron systems. *Phys. Rev. B*, 50:7757, 1994.
- [32] J. H. Oh and R. R. Gerhardtts. Self-consistent thomas-fermi calculation of potential and current distributions in a two-dimensional hall bar geometry. *Phys. Rev. B*, 56:13519, 1997.
- [33] R. R. Gerhardtts. Path-integral approach to the two-dimensional magneto-conductivity problem ii application ... *Z. Physik B*, 21:285, 1975.
- [34] R. B. Laughlin. Gauge gedankenexperiment iqhe. *Phys. Rev. B*, 23:5632, 1981.
- [35] M. Büttiker. *IBM J. Res. Dev.*, 32:317, 1988.
- [36] B. I. Halperin. Self-consistent local-equilibrium model for density profile and distribution of dissipative currents in a hall bar under strong magnetic fields. *Phys. Rev. B*, 25:2185, 1982.
- [37] E. Ahlswede, P. Weitz, J. Weis, K. von Klitzing, and K. Eberl. Hall potential profiles in the quantum hall regime measured by a scanning force microscope. *Physica B*, 298:562, 2001.
- [38] S. Ilani, A. Yacoby, D. Mahalu, and H. Shtrikman. Unexpected behavior of the local compressibility near the $b=0$ metal-insulator transition. *Phys. Rev. Lett.*, 84:3133, 2000.
- [39] G. A. Steele, R. C. Ashoori, L. N. Pfeiffer, and K. W. West. Imaging Transport Resonances in the Quantum Hall Effect. *Physical Review Letters*, 95(13):136804–+, September 2005.
- [40] K. Slevin and T. Ohtsuki. Critical exponent for the quantum Hall transition. *Phys. Rev. B*, 80(4):041304(R), July 2009.
- [41] S. Sakiroglu, U. Erkarlan, G. Oylumluoglu, A. Siddiki, and I. Sokmen. Microscopic theory of the activated behavior of the quantized Hall effect. *ArXiv e-prints:0906.0661[cond-mat.mes-hall]*, June 2009.
- [42] R. J. Haug, K. V. Klitzing, and K. Ploog. Analysis of the asymmetry in Shubnikov-de Haas oscillations of two-dimensional systems. *Phys. Rev. B*, 35:5933–5935, April 1987.
- [43] A. Siddiki and R. R. Gerhardtts. Nonlinear thomas-fermi-poisson theory of screening for a hall bar

- under strong magnetic fields. In A. R. Long and J. H. Davies, editors, *Proc. 15th Intern. Conf. on High Magnetic Fields in Semicond. Phys.*, Bristol, 2002. Institute of Physics Publishing.
- [44] R. J. Haug, R. R. Gerhardts, K. V. Klitzing, and K. Ploog. Effect of repulsive and attractive scattering centers on the magnetotransport properties of a two-dimensional electron gas. *Physical Review Letters*, 59:1349–1352, September 1987.
- [45] J. Matthews and M. E. Cage. Temperature Dependence of the Hall and Longitudinal Resistances in a Quantum Hall Resistance Standard. *J. Res. Natl. Inst. Stand. Technol.*, 110:497, October 2005.
- [46] A. Siddiki. The spin-split incompressible edge states within empirical Hartree approximation at intermediately large Hall samples. *Physica E Low-Dimensional Systems and Nanostructures*, 40:1124–1126, March 2008.